Electronic Supplementary Material (ESI) for Journal of Materials Chemistry A.

Electronic Supplementary Information (ESI) for ***Energy & Environmental Science***

Achieving an unprecedented hydrogen evolution rate by solvent-exfoliated CPP-based photocatalysis

Jing-Zhao Cheng,[a] Li-Lin Liu, [a] Guangfu Liao,[b] Zhao-Qi Shen,[a] Zhi-Rong Tan,[a] Yu-Qin Xing,[a] Kai Yang,[a] Long Chen [a] and Shi-Yong Liu*[a]

[a] School of Chemistry and Chemical Engineering, Jiangxi University of Science and Technology, Ganzhou 341000, China

[b] School of Materials Science and Engineering, PCFM Lab, GD HPPC Lab, Sun Yat-sen University, Guangzhou 510275, China.

Corresponding author:

* E-mail: chelsy@zju.edu.cn, chelsy@jxust.edu.cn (S. -Y. Liu)

Contents

Instruments and mesurements

Solid state magic angle spinning ^{13}C CP/MAS NMR measurement was carried out on a Bruker Avance 400 model 400 MHz NMR spectrometer at a MAS rate of 10 kHz. FT-IR spectrum was measured on a FT-IR spectrometer (Bruker, ALPHA) in transmission mode at room temperature. Thermal properties of the polymer networks were evaluated using thermogravimetric analysis (TGA) with a differential thermal analysis instrument (STA2500, NETZSCH) over the temperature range from 30 to 800 °C under a nitrogen atmosphere with a heating rate of 10 ℃ min^{-1}. Elemental analysis was measured by a Vario MICRO.

Pd and Sn contents were determined by inductively coupled plasma optical emission spectrometry (ICP-OES, IRIS Intrepid Ⅱ), where the sample was digested in HNO_3/HCl (1/1, v/v) at 265 ℃, then raised the temprature to 300 ℃, added $HClO_4$, then added HNO_3 to extract after steaming, and diluted it by ultrapure water and filtered.

X-ray photoelectron spectroscopy (XPS) measured by Thermo ESCALAB 250XI instrument. Morphology of CPPs was obtained by a field emission scanning electron microscope (SEM, MLA650F, American) and transmission electron microscopy (TEM, Tecnai G2-20, American). Thickness of the solvent-exfoliated CPPs was characterized by a Bruker Multimode 8 atomic force microscope (AFM) under Scan Asyst mode (Bruker, USA). Specific surface areas were determined by a Tristar II 3020 (Micromeritics, Norcross, Georgia) with nitrogen as analytical gas. Samples were degassed under vacuum at ambient temperature for 24 h. The volume of nitrogen adsorption was recorded over a relative pressure range between 0.01 and 0.99. 8 points in the relative pressure range of 0.05–0.2 were used for the calculation of the surface area according to the Brunauer-Emmet-Teller (BET) theory. Contact angle were obtained by JCY type measurement instrument. (Shanghai Fang Rui Instrument Co. Ltd.)

UV-vis diffuse reflectance spectra were carried out on UV-2600 scanning UV-vis spectrophotometer. Time-resolved fluorescence spectroscopy and photoluminescence (PL) spectra were obtained on HORIBA Instruments FL-1000 fluorescence spectrometer. The photocurrents were measured by an electrochemical workstation (CHI650E/700E, Shanghai) equipped with a conventional three-electrode cell. Cyclic voltammetry (CV) measurement was carried out on a CHI660E (Chenhua, Shanghai) electrochemical workstation in a three electrode-cell system: Ag/Ag^+ work as the reference electrodes, glassy carbon electrodes as the working electrode, t platinum wire work as the counter electrode. The tetrabutylammonium hexafluorophosphate (Bu_4NPF_6, 1.5 g) dissolved in 5 mL acetonitrile was used as the electrolyte solution. The electrochemical workstation was taken with a scan rate of 100 mV s^{-1} in the range of –2.5 V to 2.5 V and two times. Before the electrochemical test, CPP (2 mg) was dispersed in ethanol and then pipet 5uL of the mixed solution onto the working electrode. After the ethanol was air-dried, 5 uL of chitosan was added to deposit the sample on the electrode. Theoretical calculations based on DFT methods have been performed for the oligomers with Gaussian09 program. Becke's three-parameter gradient-corrected functional (B3LYP) with 6-31G(d,p) basis for geometric optimization.

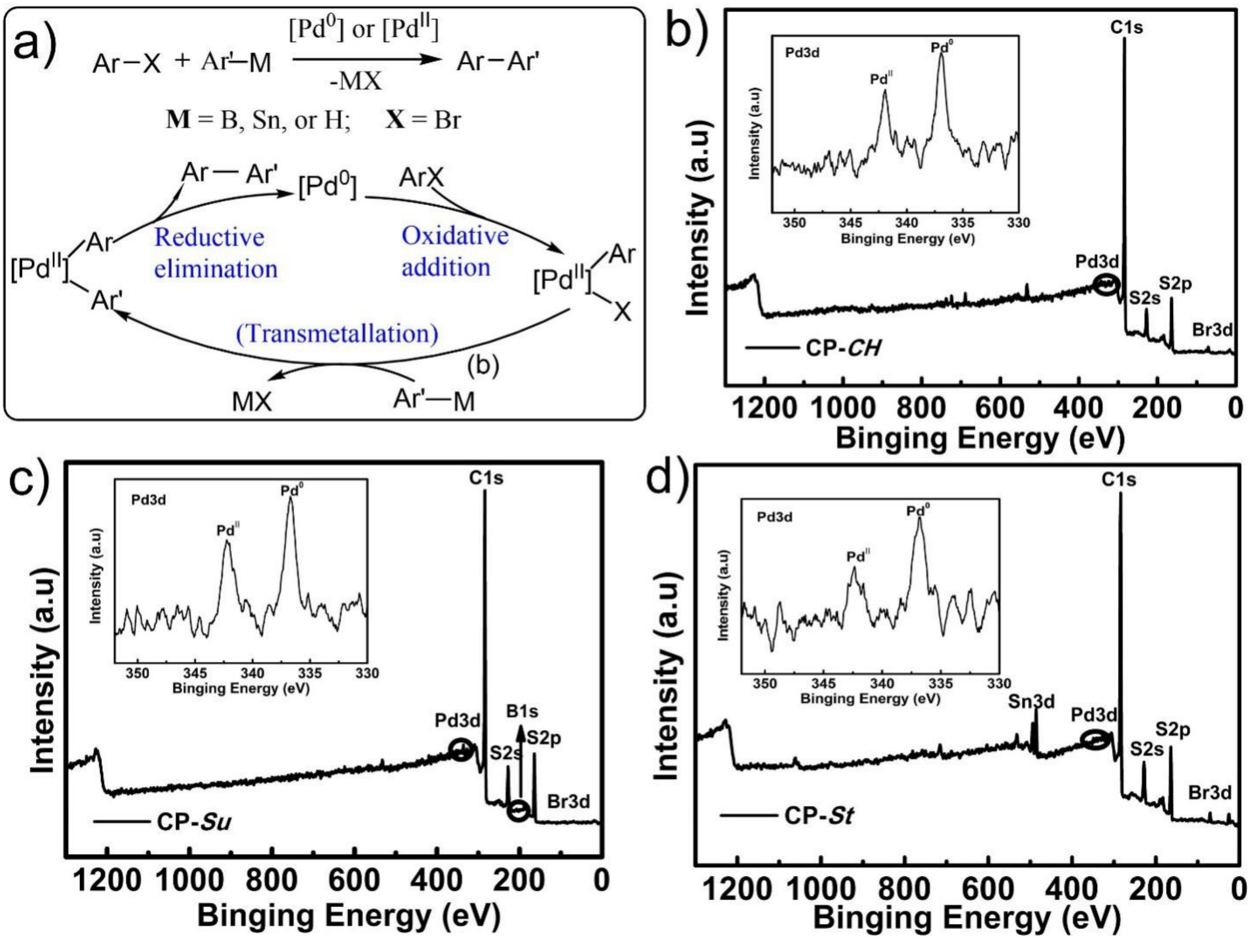

Fig. S1 Catalytic cycle of Pd-catalyzed C-M/C-Br (M=B, H and Sn) couplings that involves Pd^0 Pd^{II} interchange (a), XPS spectra of **CP-*CH*** (b), **CP-*Su*** (c) and **CP-*St*** (d), and inserts are Pd3d.

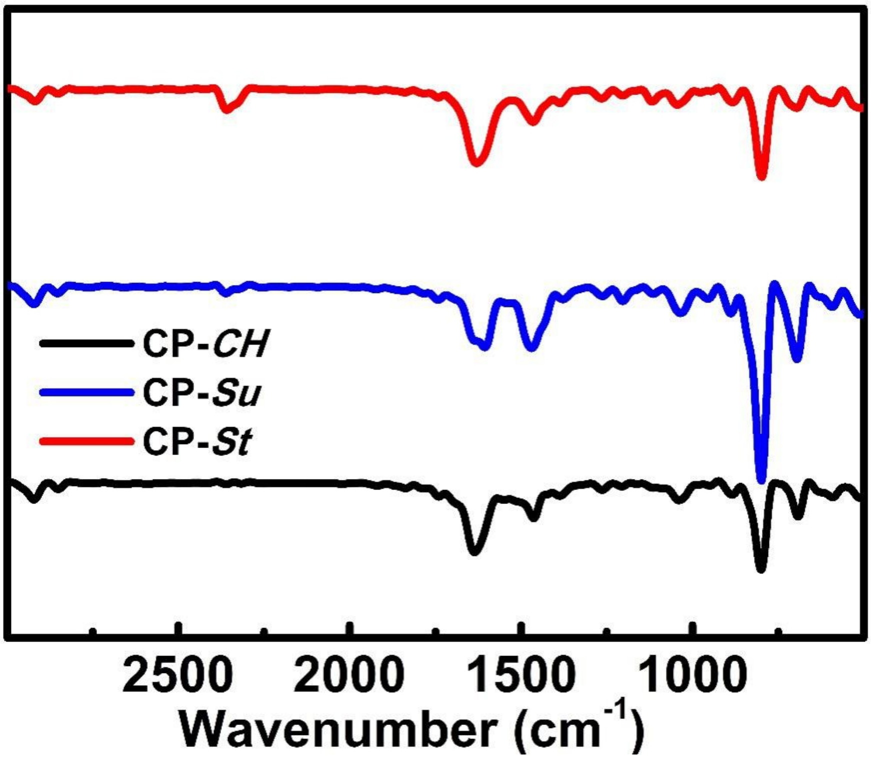

Fig. S2 FT-IR spectra of as-prepared **CP-*CH***, **CP-*Su*** and **CP-*St***

[The peaks at 1626 cm^{-1} and 1466 cm^{-1} were the skeleton vibration of the aromatic ring for all polymers. The signal at 808 cm^{-1} was the C−S stretching vibration from thiophene units.]

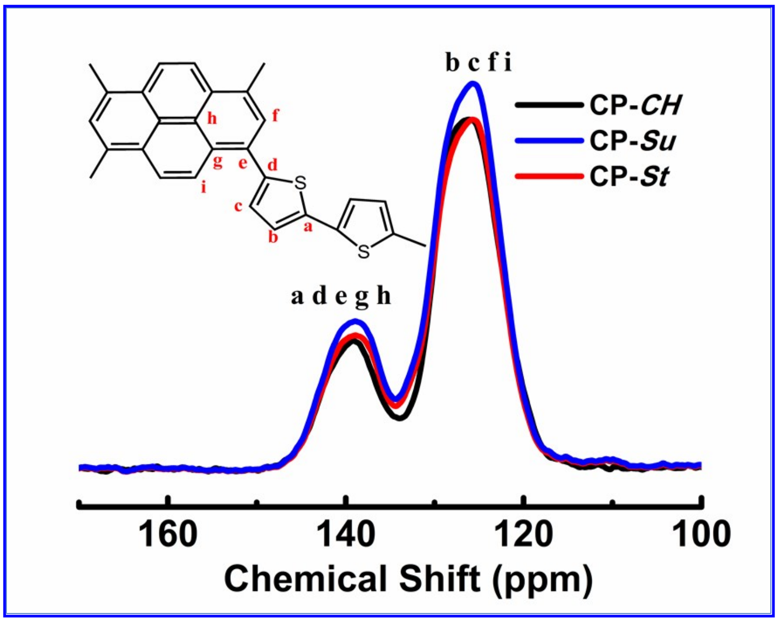

Fig. S3 Solid-state ^{13}C NMR spectrum of **CP-*CH***, **CP-*Su*** and **CP-*St*.**

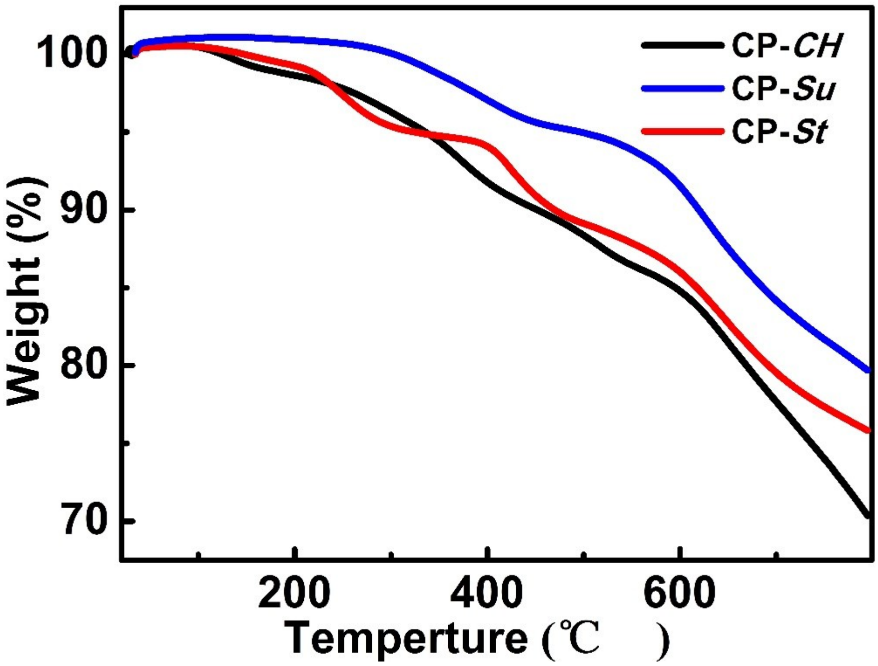

Fig. S4 TGA curves of as-prepared **CP-*CH*** , **CP-*Su*** and **CP-*St*.**

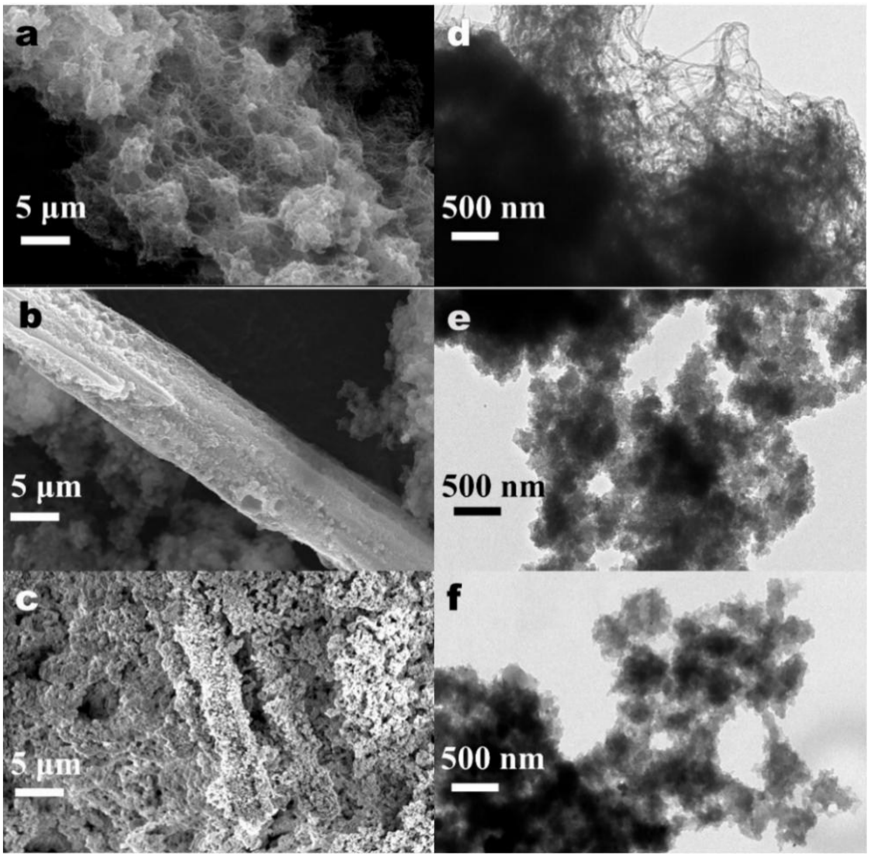

Fig. S5 SEM and TEM images of **CP-*CH*** (a, d), **CP-*Su*** (b, e) and **CP-*St*** (c, f).

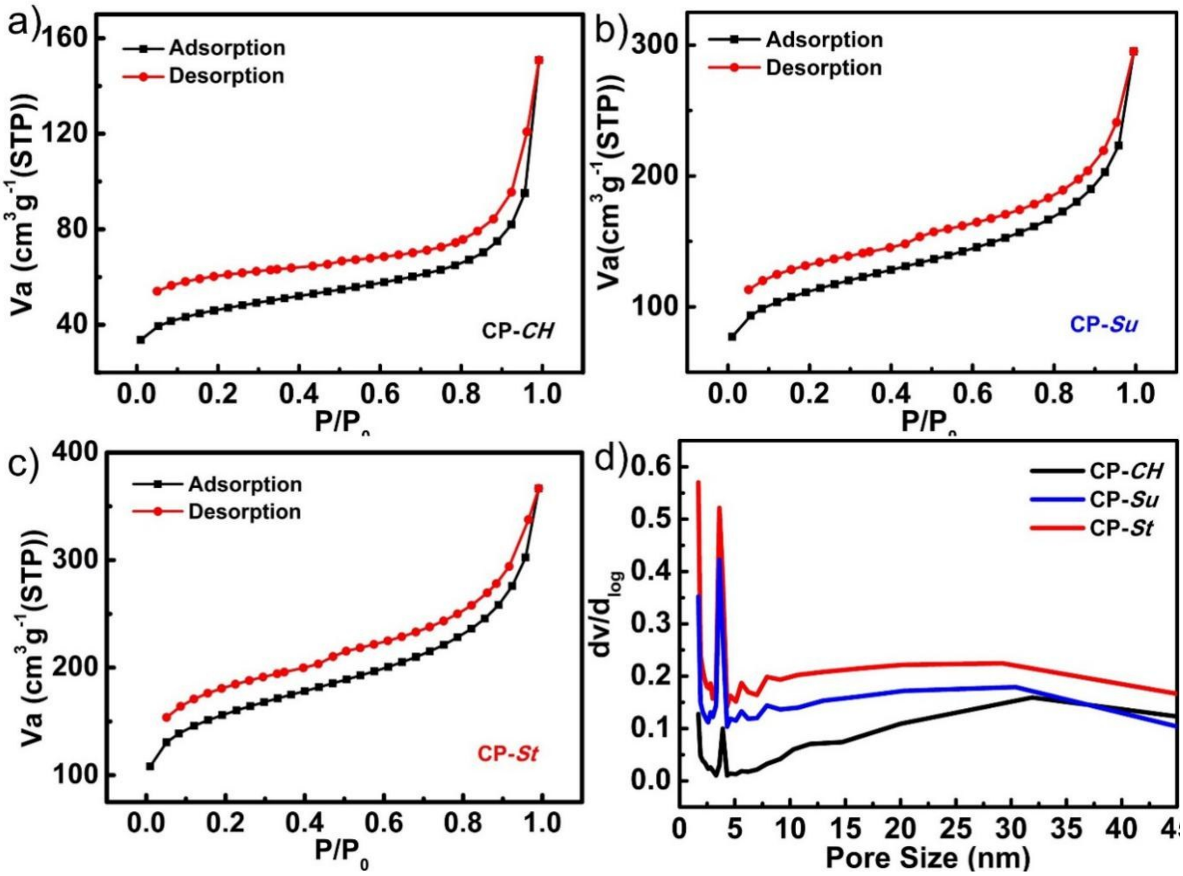

Fig. S6 N_2 adsorption-desorption isotherms of **CP-*CH***, **CP-*Su*** and **CP-*St*** (a~c) and their pore size distribution (d).

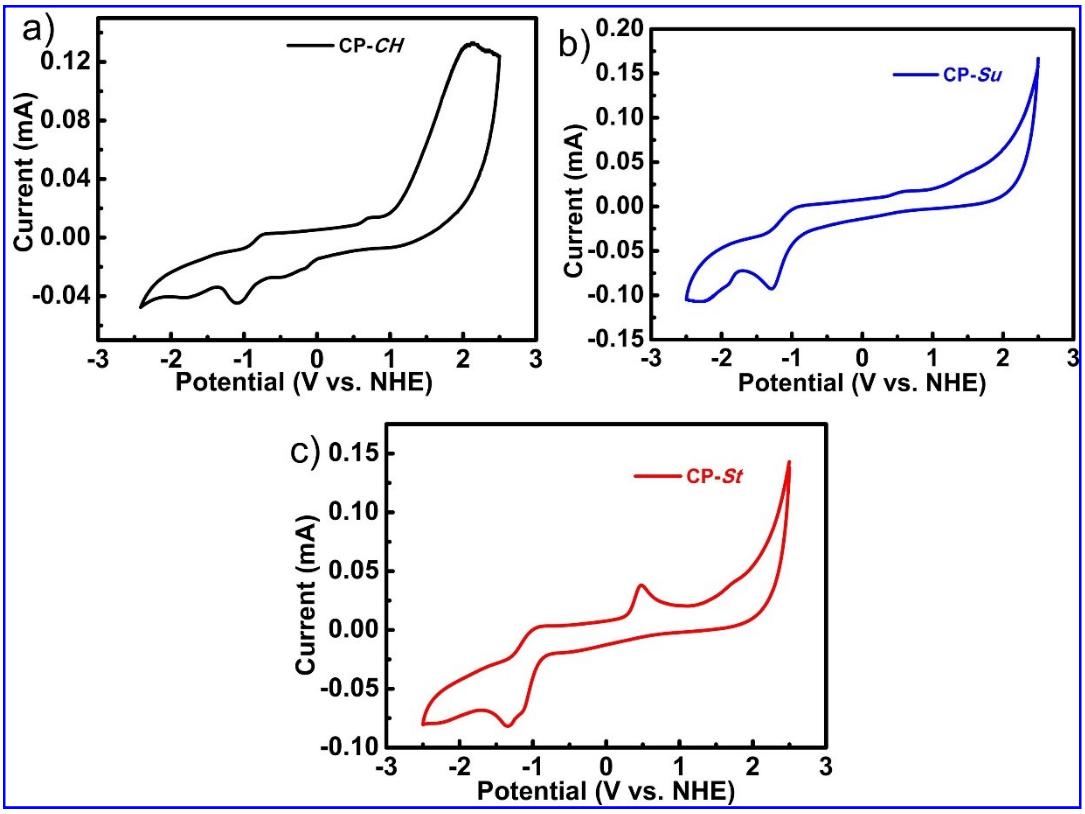

Fig. S7 CV curves of **CP-*CH***, **CP-*Su*** and **CP-*St***.

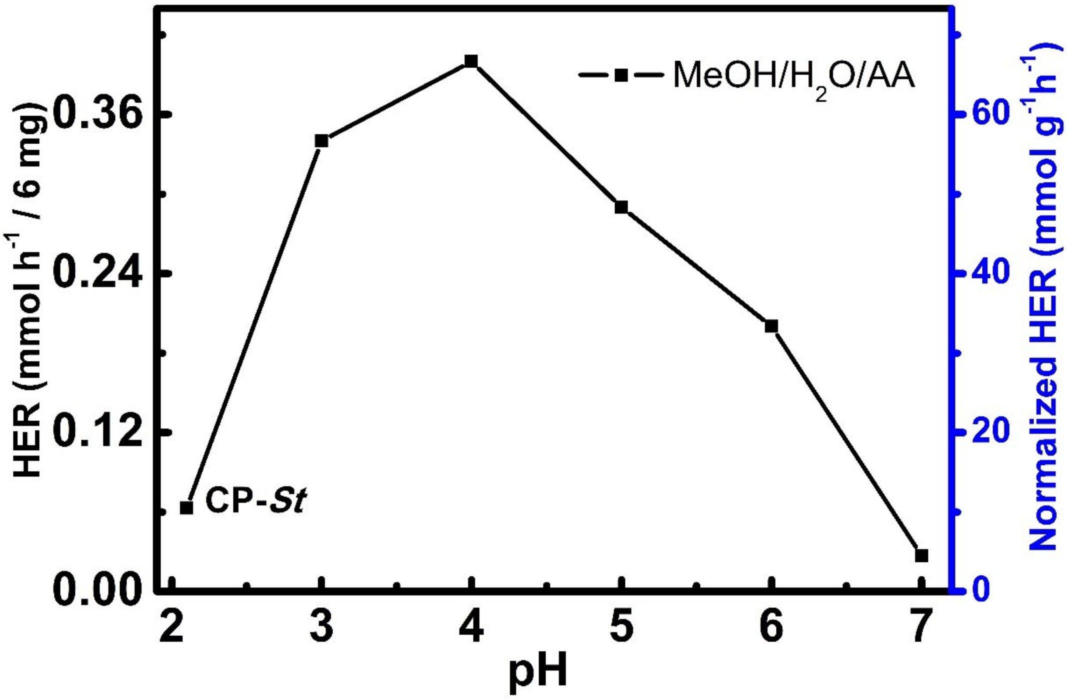

Fig. S8 Influences of pH on the PHP activity of **CP-*St***/MeOH/H_2O/AA mixture (λ >420)

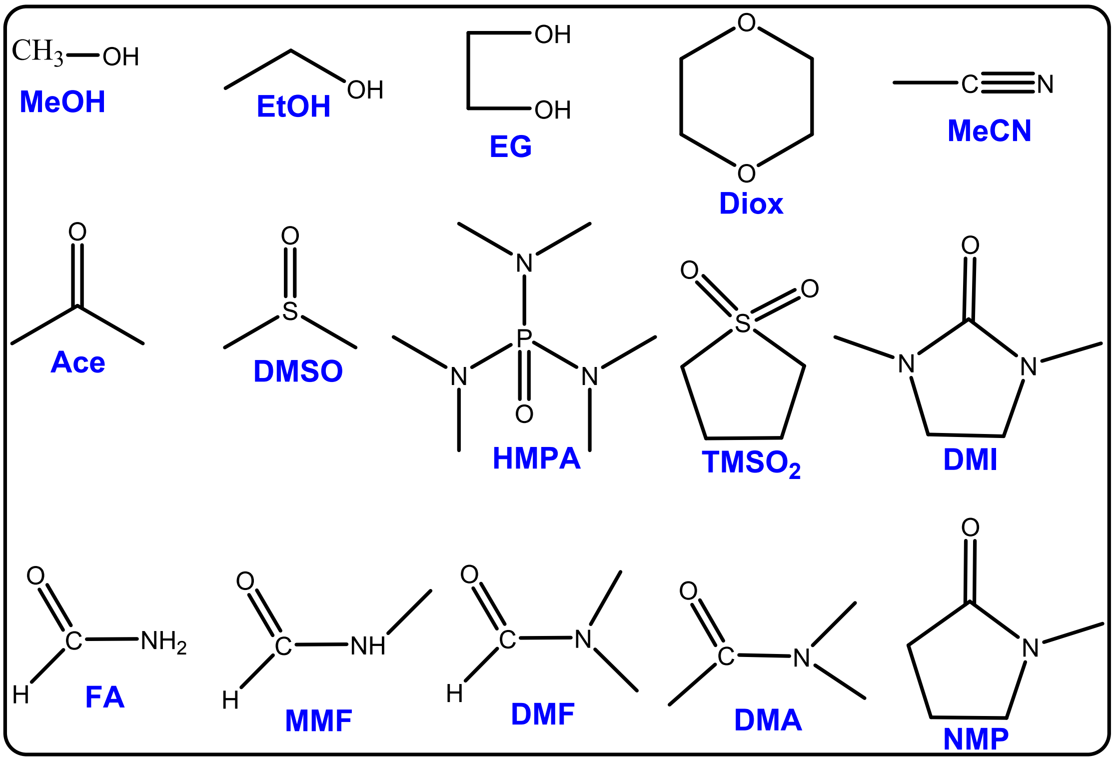

Fig. S9 Molecular structures of 15 co-solvents investigated in this work.

Table S1 PHP activity of **CP-*St*** (6 mg) in varied reaction media (pH=4) using AA as SED.

Entry	Mixed solvent	H_2 amount (mL)	HER (mmol h^{-1} / 6mg)	TON	HER (mmol h^{-1} g^{-1})
1	H_2O	6.7	0.06	26	10.0
2	EG/H_2O	9.6	0.09	38	14.3
3	EtOH/H_2O	13.7	0.12	55	20.3
4	Diox/H_2O	40.3	0.36	158	60.0
5	Ace/H_2O	43.7	0.39	171	65.0
6	MeOH/H_2O	44.6	0.40	175	66.3
7	HMPA/H_2O	58.9	0.53	231	87.7
8	FA/H_2O	63.4	0.57	248	94.3
9	$TMSO_2$/H_2O	67.2	0.60	263	100.0
10	MeCN/H_2O	67.9	0.61	266	101.0
11	DMSO/H_2O	70.6	0.63	276	105.0
12	MMF/H_2O	88.3	0.79	345	131.3
13	DMI/H_2O	112.4	1.00	440	**167.3**
14	DMF/H_2O	119.6	1.07	468	**178.0**
15	DMAc/H_2O	120.1	1.07	470	**178.7**
16	NMP/H_2O	128.1	**1.14**	502	**190.7**

Refs.	SED	With Pt or not?	Light source		HER [μmmol h^{-1} / amount of catal. (mg)]	Normalized HER (μmmol h^{-1} g^{-1})	Catalyst	AQY (%)
			Filter (nm)	Power(W)				
1.	TEOA	---	>420	300 (Xe)	947/50	18,940	CN-NS	26.1
2.	TEOA	3%	>420	300 (Xe)	770/50	15,400	g-CN	50.7
3	AA	---	>420	17(LED)	--	50,000	PFODTBT	0.6
4	TEOA	3%	>420	300 (Xe)	442/10	44,200	PDBTSO	--
5	TEA	3%	>420	300 (Xe)	1874/50	37,480	DACN-100	34.4
6	MeOH& TEA	3%	>420	300 (Xe)	19.7/0.325	84,000	P10-e	20.4
7	TEOA	3%	>300	300 (Xe)	649.3/50	12,986	PyDOBT-1	6.1
8	AA	0.1% Pt	>420	17(LED)	16.25	50,000	PS-PEG-COOH	0.5
9	lactic acid	---	>420	300 (Xe)	6415	128,300	Pt/TiO2/CdS	--
10	glycerol	3.8%	>420	230 (LED)	--	70,800	TiO_2/rGO(3%)	--
11	TEOA	3%	>420	300 (Xe)	460/50	9200	DBTD-CMP1	3.3
12	TEA	---	>420	300 (Xe)	81.5/25	3260	P10	11.6
13	AA	With Pt	>420	300 (Xe)	815/5	16,300	FS-COF	3.2
This work	AA	---	>420	300 (Xe)	1140/6	190,700	**CP-*St***	**6.9**
This work	AA	---	>420	300 (Xe)	1720/12	143,000	**CP-*St***	**9.6**
This work	AA	---	>420	300 (Xe)	1900/18	105,400	**CP-*St***	**11.4**
This work	AA	0.5%	>420	300 (Xe)	1820/6	307,200	**CP-*St***	**--**

1. G. Liu, T. Wang, H. Zhang, X. Meng, D. Hao, K. Chang, P. Li, T. Kako and J. Ye, *Angew. Chem. Int. Ed.*, 2015, **54**, 13561.

2. L. Lin, H. Ou, Y. Zhang and X. Wang, *ACS Catal.*, 2016, **6**, 3921.

3. P. B. Pati, G. Damas, L.Tian, D. L. A. Fernandes, L. Zhang, I. B. Pehlivan, T. Edvinsson, C. M. Araujo and H. Tian, *Energy Environ. Sci.*, 2017, **10**, 1372.

4. G. Shu, Y. Li, Z. Wang, J. X. Jiang and F. Wang, *Appl. Catal. B Environ.*, 2020, **261**, 118230.

5. Q. Han, Z. Cheng, B. Wang, H. Zhang and L. Qu, *ACS Nano*, 2018, **12**, 5221.

6. C. M. Aitchison, R. S. Sprick and A. I. Cooper, *J. Mater. Chem. A*, 2019, **7**, 2490.

7. Y. Zhao, W. Ma, Y. Xu, C. Zhang, Q. Wang, T. Yang, X. Gao, F. Wang, C. Yan and J. X. Jiang, *Macromolecules*, 2018, **51**, 9502.

8. L. Wang, R. F.-Terán, L. Zhang, D. L. A. Fernandes, L. Tian, H. Chen and H. Tian, *Angew. Chem. Int. Ed.*, 2016, **55**, 12306.

9. J. Wang, Z. Wang, P. Qu, Q. Xu, J. Zheng, S. Jia, J. Chen and Z. Zhu, *Int. J. Hydrogen Energy*, 2018, **43**, 7388.

10. P. Ribao, M. A. Esteves, V. R. Fernande, M. J. Rivero, C.M. Rangel and I. Ortiz, *Hydrogen Energy*, 2019, **44**, 28494.

11. Z. Wang, X. Yang, T. Yang, Y. Zhao, F. Wang, Y. Chen, J. H. Zeng, C. Yan, F. Huang and J. X. Jiang, *ACS Catal.*, 2018, **8**, 8590.

12. M. Sachs, R. S. Sprick, D. Pearce, S. A. J. Hillman, A. Monti, A. A. Y. Guilbert, N. J. Brownbill, S. Dimitrov, X. Shi, F. Blanc, M. A. Zwijnenburg, J. Nelson, J. R. Durrant and A. I. Cooper, *Nat. Commun*, 2018, **9**, 4968.

13. X. Wang, L. Chen, S. Y. Chong, Y. Wu, W. H. Zhu, M. A. Zwijnenburg, R. S. Sprick and A. I. Cooper, *Nat. Chem.*, 2018, **10**, 1180.

Table S2 Summary of publised HER and the normalized HERs of organic & inorganic photocatalysts.

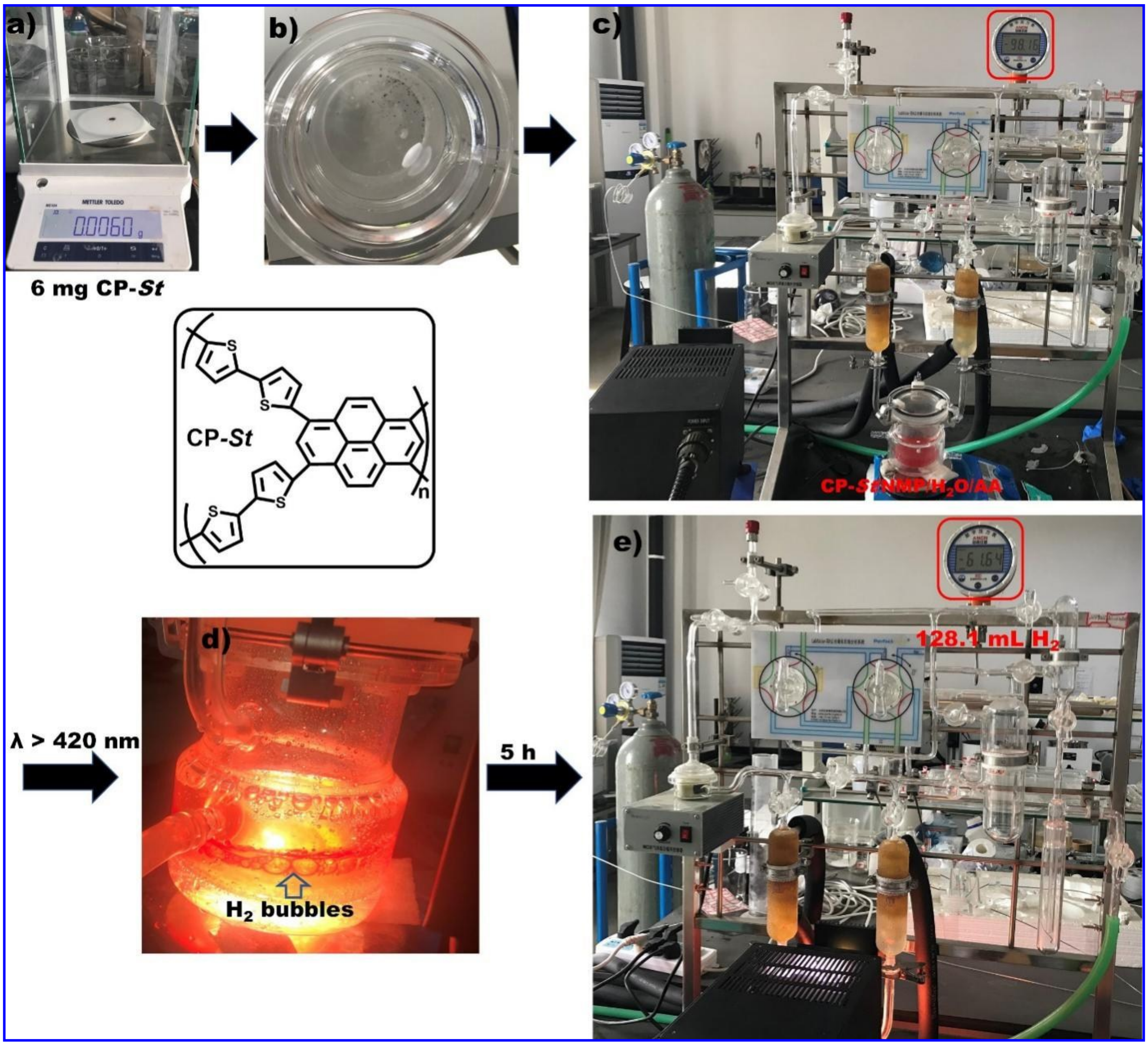

Fig. S10 6.0 mg **CP-*St*** (a) put in reaction vessel (b), and dispersed in NMP/H_2O/AA mixed solution (36 mL, pH =4), before (c), during (d) and after (e) irradiation under visible light for 5 h. [The amount of H_2 were checked by the GC equipped with a TCD detector, the reading on vacuum gauge before and after irradiation are shown in c and e]

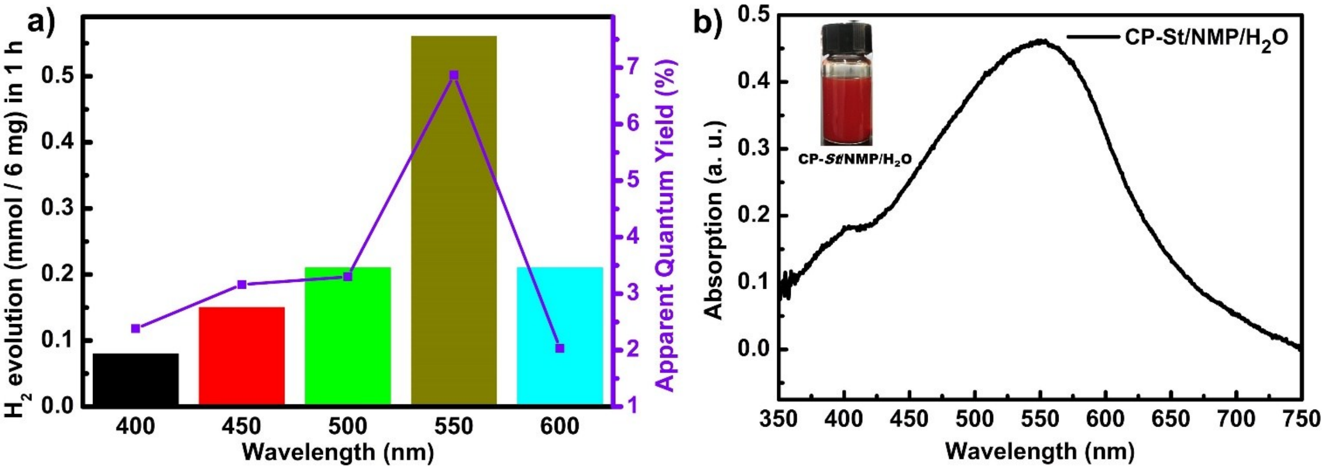

Fig. S11 (a) The hydrogen evolutions (mmol) of **CP-*St*** (6 mg) dispersed in NMP/H_2O/AA (pH=4) under different monochromatic light irradiation in 1 h, and their corresponding AQY values. (b) Uv-vis spectrum of dispersion of **CP-*St*** in NMP/H_2O mixed solvent (insert is its corresponding digital photo).

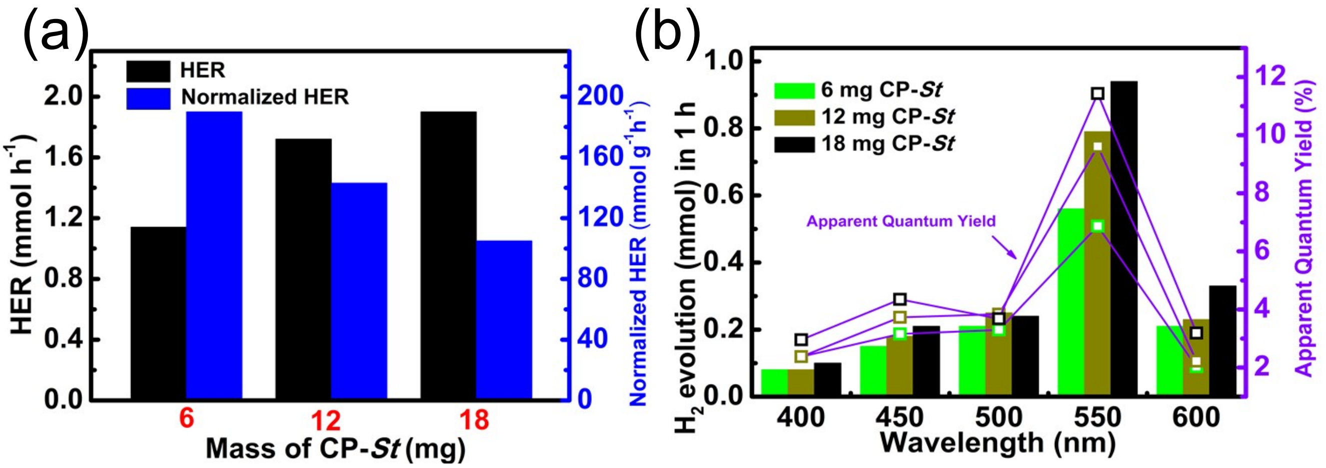

Fig. S12 Influence of mass of **CP-*St*** dispersed in NMP/H_2O/AA on the HERs under visible light (a), and AQYs (b).

[6, 12 and 18 mg **CP-*St*** were dispersed in 36 mL NMP/H_2O/AA solution (6 mL NMP + 30 mL H_2O + 4 g AA) with a pH adjusted to 4, and subjected to HER and AQY test, respectively. It was found that the un-normalized HERs did not linearly increase with the increase of masses of **CP-*St*** used. As a resut, 18 mg **CP-*St*** has the highest un-normalized HER (mmol h^{-1}) and highest AQY, while a lowest normalized HER (mmol h^{-1} g^{-1}).]

Table S3 HERs and AQYs of varied masses of **CP-*St*** dispersed in NMP/H_2O/AA solution[a]

Mass (mg)	HER (mmol h^{-1}) [b]	Normalized HER (mmol $h^{-1}g^{-1}$) [b]	Wavelength (nm)	H_2 evolution (mmol) in 1 h	AQY (%)
6	1.14	190.7	400	0.08	2.38
			450	0.15	3.16
			500	0.21	3.3
			550	**0.56**	**6.87**
			600	0.21	2.03
12	1.72	143.0	400	0.08	2.38
			450	0.18	3.73
			500	0.25	3.84
			550	**0.79**	**9.61**
			600	0.23	2.22
18	1.90	105.4	400	0.10	2.96
			450	0.21	4.35
			500	0.24	3.68
			550	**0.94**	**11.43**
			600	0.33	3.19

[a] All varied masses of CP-St were dispersed in 36 mL NMP/H_2O/AA solution (6 mL NMP + 30 mL H_2O + 4 g AA) with a pH adjusted to 4. [b] Under visible light irradiation (λ>420 nm).

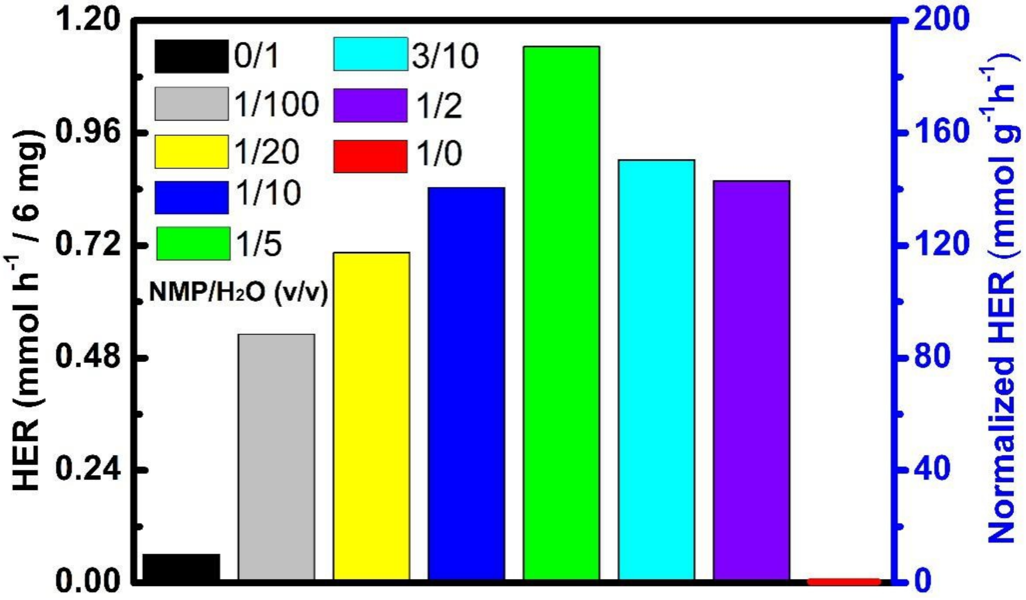

Fig. S13 Influence of amount of NMP on the HERs of **CP-*St***/NMP/H_2O/AA mixture.

Table S4 The influence amount of NMP on the HERs of **CP-*St***/NMP/H_2O/AA mixture.

Entry	NMP/H_2O (v/v)	H_2 evolution (mL)	HER (mmol ^{1}h^{-1} /6 mg)	TON	HER (mmol h^{-1}g^{-1})
1	0/1	6.7	0.06	26	10.0
2	1/100	59.4	0.53	233	88.4
3	1/20	78.9	0.70	309	117.4
4	1/10	94.5	0.84	370	140.6
5	1/5	128.1	**1.14**	502	**190.7**
6	3/10	101.1	0.90	396	150.4
7	1/2	96.0	0.86	378	142.9
8 [a)]	1/0	0	0	0	0
9 [b)]	1/5	0	0	0	0
10 [c)]	1/5	0	0	0	0

[a)] In the absence of water.

[b)] **CP-*St***/NMP/H_2O/AA mixture under darkness.

[c)] NMP/H_2O/AA mixture under light irradiation in the absence of photocatalyst.

Table S5 The correlation between PHP activity and structure & properties of varied cosolvents using **CP-*St*** and AA as catalyst and SED, respectively. [a)]

Reaction media	Hydrogen bonding donor	Hydrogen bonding acceptor	HER (mmol $h^{-1}g^{-1}$)
EG/H_2O	strong	middle	14.3
EtOH/H_2O	strong	middle	20.3
Diox/H_2O	no	middle	60.0
Ace/H_2O	weak	strong	65.0
MeOH/H_2O	strong	middle	66.3
HMPA/H_2O	no	strong	87.7
FA/H_2O	middle	strong	94.3
$TMSO_2$/H_2O	no	strong	100.0
MeCN/H_2O	weak	strong	101.0
DMSO/H_2O	no	strong	105.0
MMF/H_2O	weak	strong	131.3
DMI/H_2O	no	strong	**167.3**
DMF/H_2O	no	strong	**178.0**
DMAc/H_2O	no	strong	**178.7**
NMP/H_2O	no	strong	**190.7**

[a)] HERs increase from up to down.

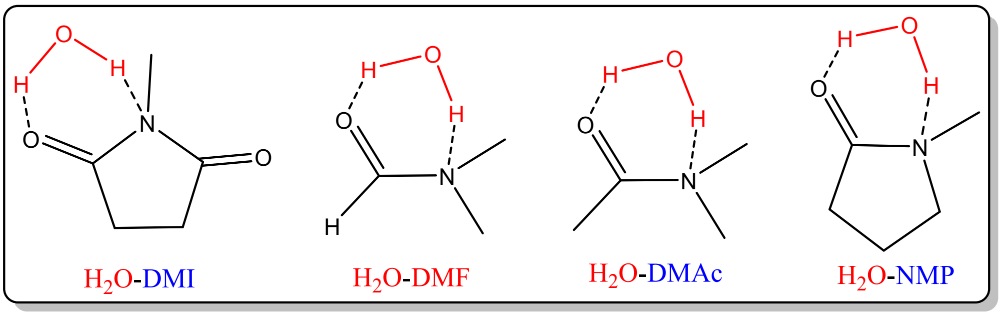

Scheme S1 Non-covalent interaction between water-soluble aprotic bipolar solvents (reaction media) and the protons of H_2O.

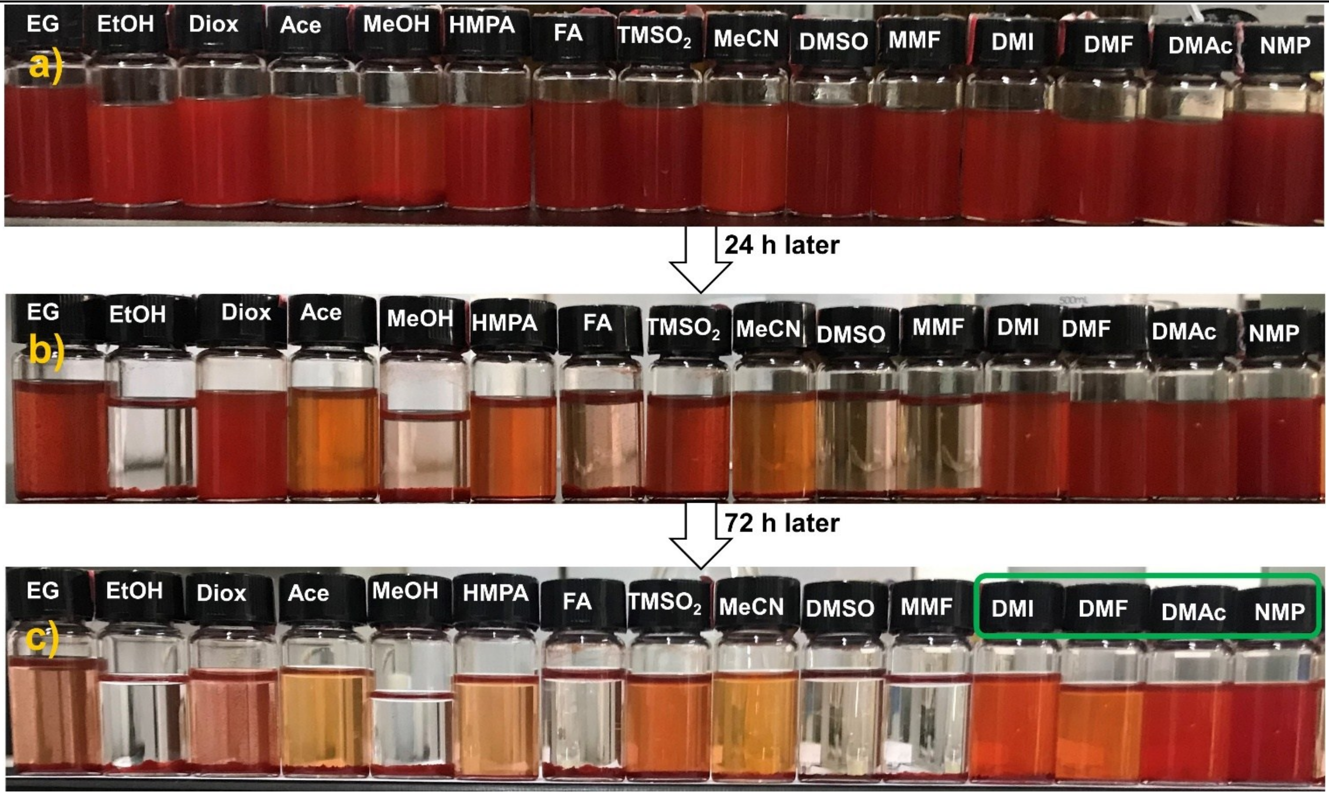

Fig. S14 CP-*St* ultrasonically dispersed (for 10 minutes) in varied solvents, and standing for 0 h (a), 24 h (b) and 72 h (c), respectively.

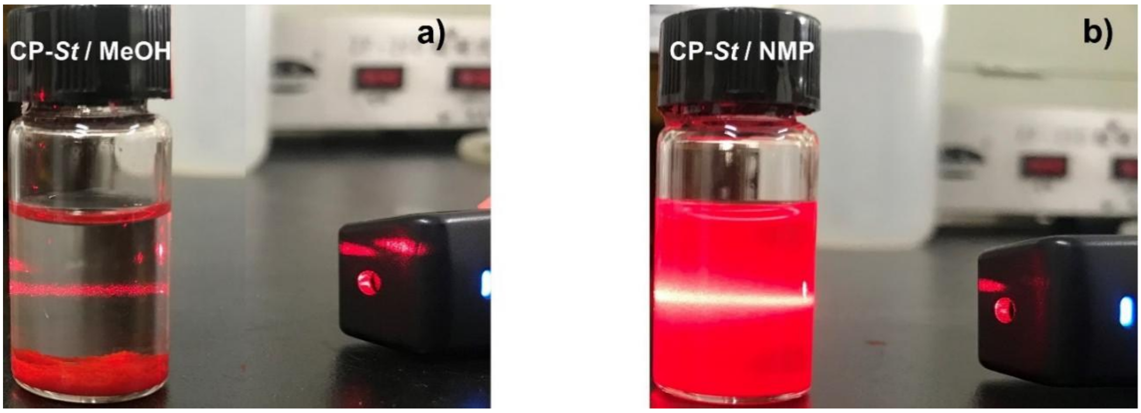

Fig. S15 Light beams pass through the stored dispersions of **CP-*St*** in MeOH (a) and NMP (b). [(b) shows the Tyndall effect of **CP-*St*** dispersed in NMP after being store for one month.]

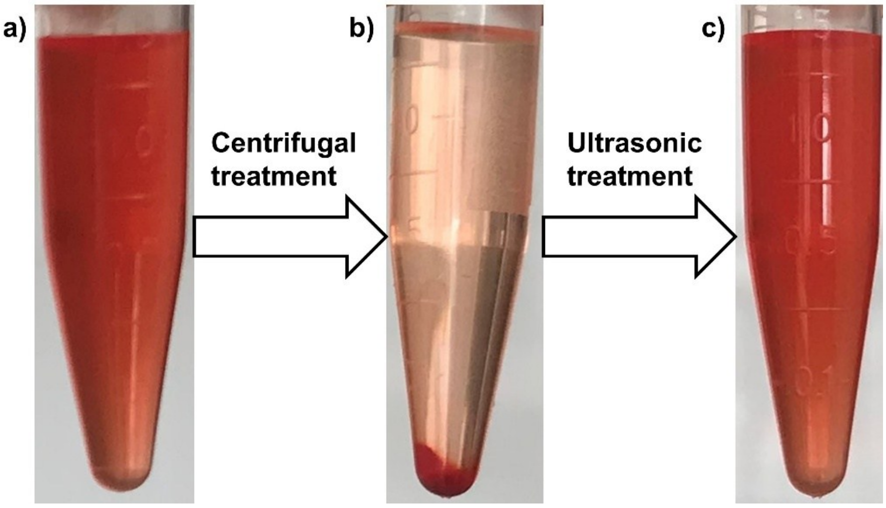

Fig. S16 Dispersion of **CP-*St*** in NMP after being stored for one month (a), then treated by centrifugation at a speed of 10,000 r. p. m. (b), and re-dispersed by a conventional ultrasonic treatment (c).

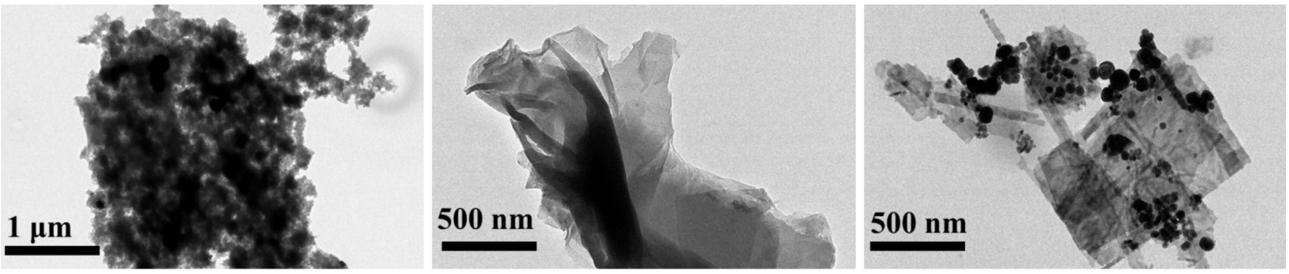

Fig. S17 TEM images of bulk **CP-*St*** (a), and **CP-*St*** exfoliated by NMP (b) (c) and (d).
[The TEM samples of bulk and exfoliated ones were obtained by dropping EtOH and NMP dispersions, respectively, onto carbon grids]

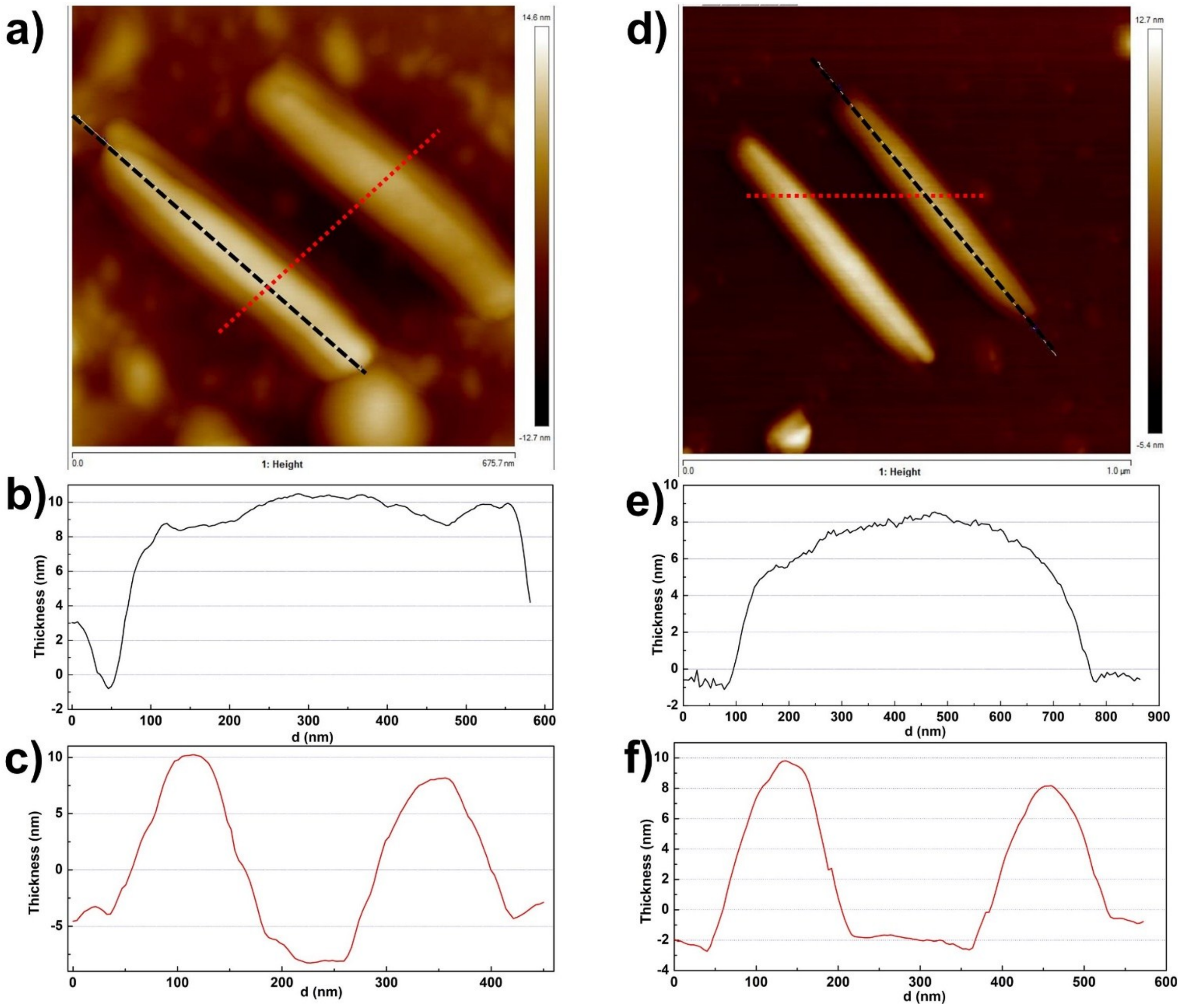

Fig. S18 AFM images of **CP-*St*** nanosheets exfoliated by DMF (a) and NMP (d) and corresponding thickness analysis ((b), (c), and (e) and (f).

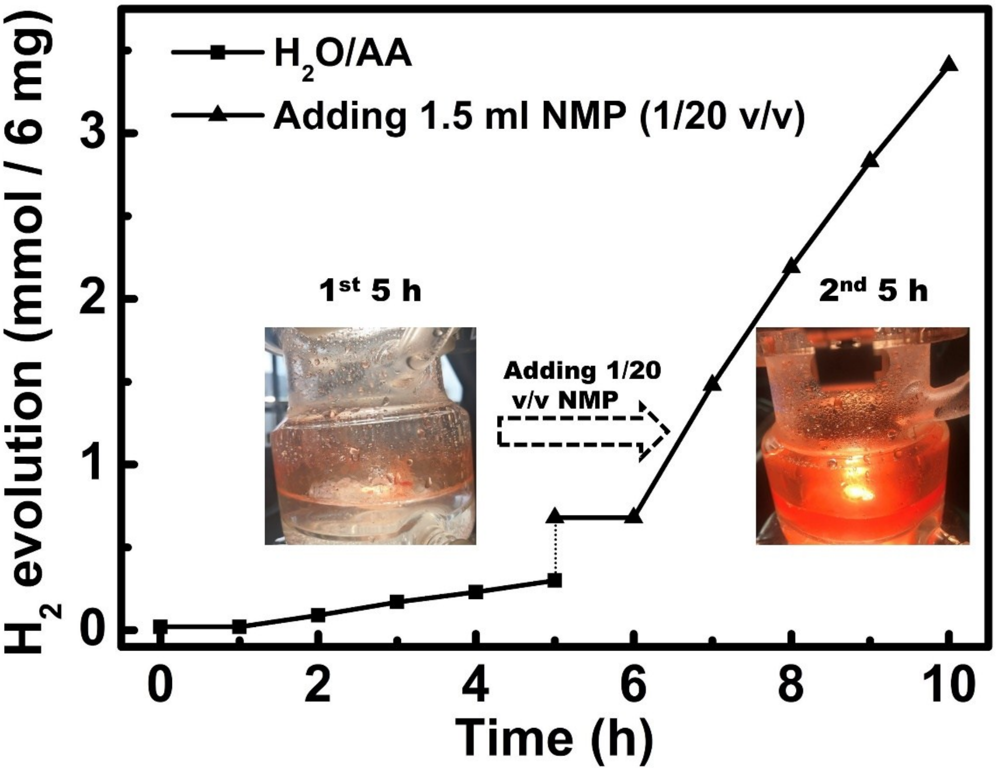

Fig. S19 The influence of introduction of NMP into **CP-*St***/H_2O/AA mixture on PHP activity.

[**CP-*St*** dispersed in H_2O/AA was subjected to visible-light irradiation for the first 5 h, then stopped it, added a small amount of NMP (1/20 v/v) into the reaction mixture, and restarted it for the next 5 h.]

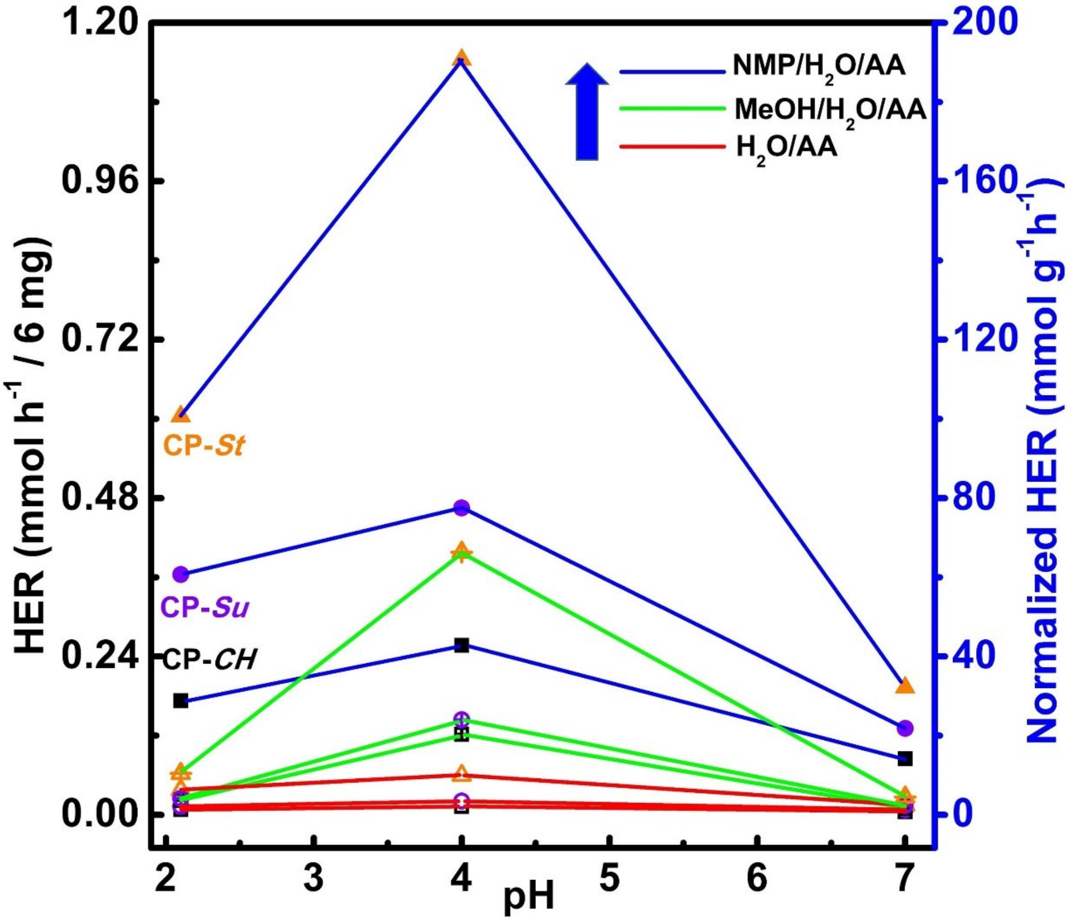

Fig. S20 The HERs of **CP-*CH***, **CP-*Su*** and **CP-*St*** dispersed in H_2O/AA, MeOH/H_2O/AA and NMP/H_2O/AA at pHs 2.1, 4.0 and 7.0, respectively.

Table S6. The HERs of **CP-*CH***, **CP-*Su*** and **CP-*St*** dispersed in H_2O/AA, MeOH/H_2O/AA and NMP/H_2O/AA at pHs 2.1, 4.0 and 7.0, respectively.

CPPs	**Solvent**	**pH=2.1**		**pH=4**		**pH=7**	
		HER (mmol h^{-1}) 6 mg CP	Normalized HER (mmol h^{-1} g^{-1})	HER (mmol h^{-1}) 6 mg CP	Normalized HER (mmol $h^{-1}g^{-1}$)	HER (mmol h^{-1}) 6 mg CP	Normalized HER (mmol h^{-1} g^{-1})
CP-*CH*	H_2O	0.008	1.4	0.013	2.2	0.005	0.9
	MeOH/H_2O	0.022	3.7	0.122	20.4	0.040	6.7
	NMP/H_2O	0.173	28.9	0.257	42.9	0.085	14.1
CP-*Su*	H_2O	0.013	2.2	0.021	3.4	0.008	1.4
	MeOH/H_2O	0.025	4.2	0.144	24.0	0.038	6.3
	NMP/H_2O	0.364	60.7	0.465	77.5	0.131	21.9
CP-*St*	H_2O	0.038	6.3	0.060	10.0	0.015	2.5
	MeOH/H_2O	0.063	10.5	0.398	66.4	0.054	9.1
	NMP/H_2O	0.604	100.7	**1.144**	**190.7**	0.193	32.1

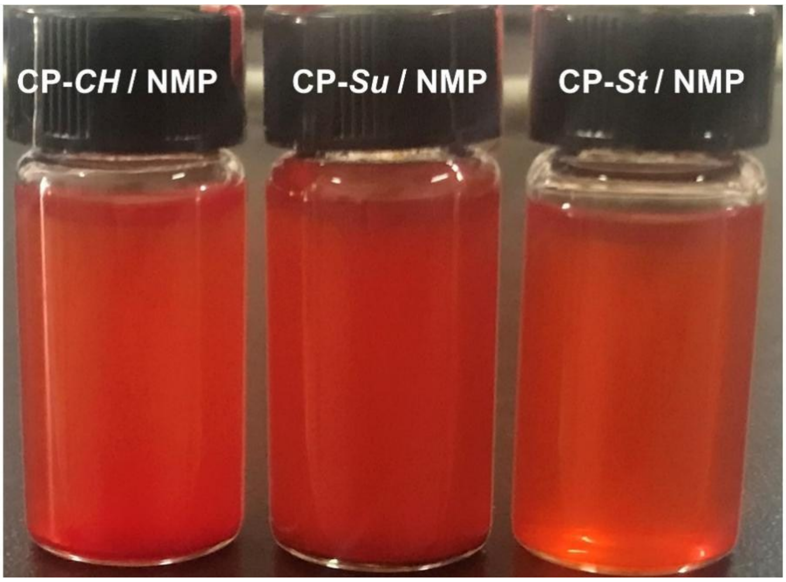

Fig. S21 CP-*CH*, **CP-*Su*** and **CP-*St*** ultrasonically dispersed in NMP, and standed for one week.

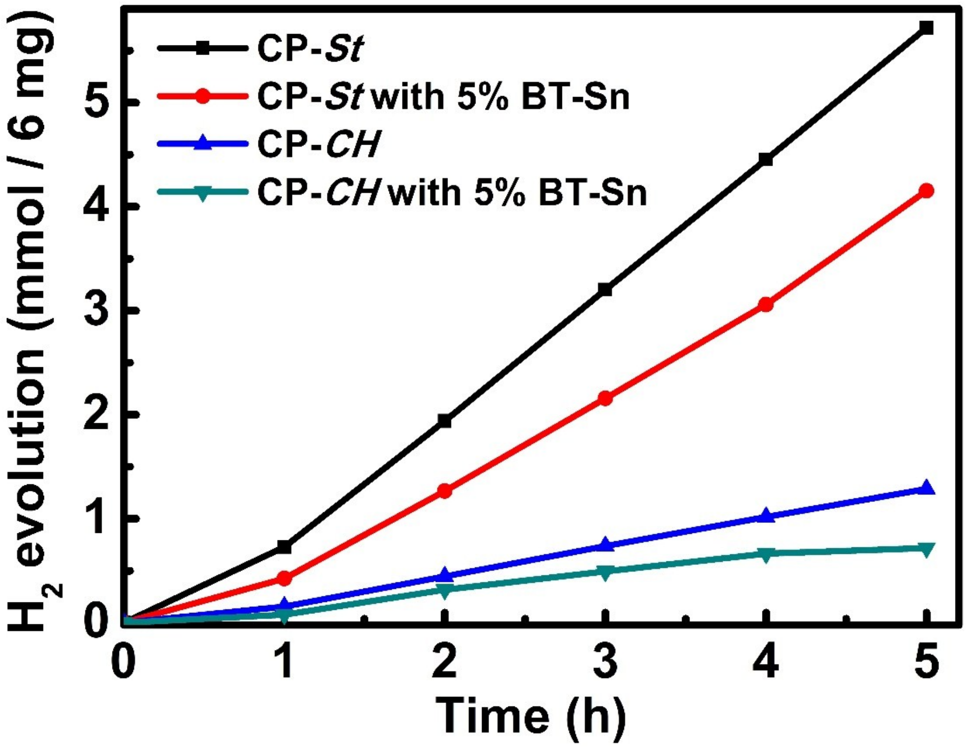

Fig. S22 HERs of **CP-*St*** and **CP-*CH*** in NMP/H_2O/AA with and without BT-Sn.

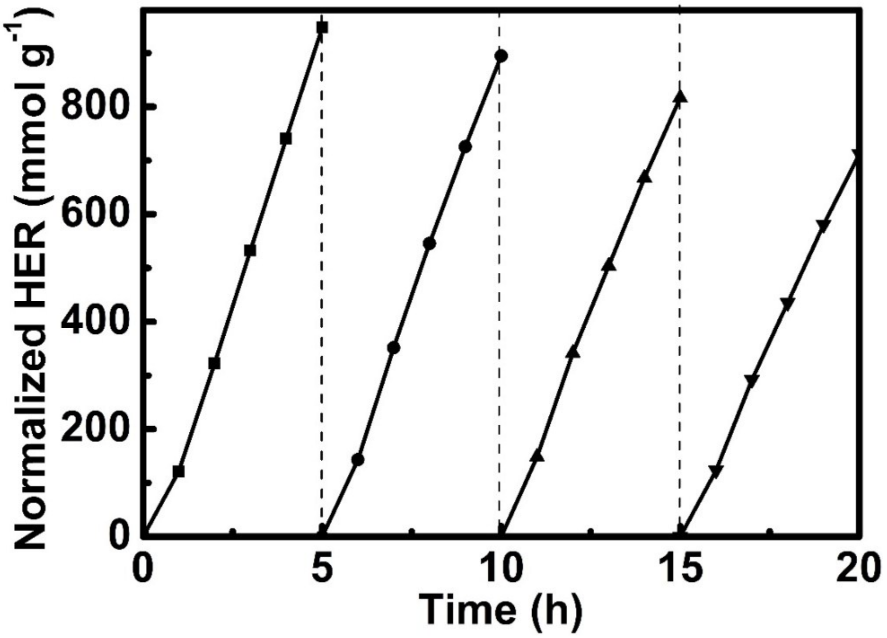

Fig. S23 Cycling test of H_2 evolution (evacuation every 5 h) for **CP-*St***/NMP/H_2O/AA mixture.

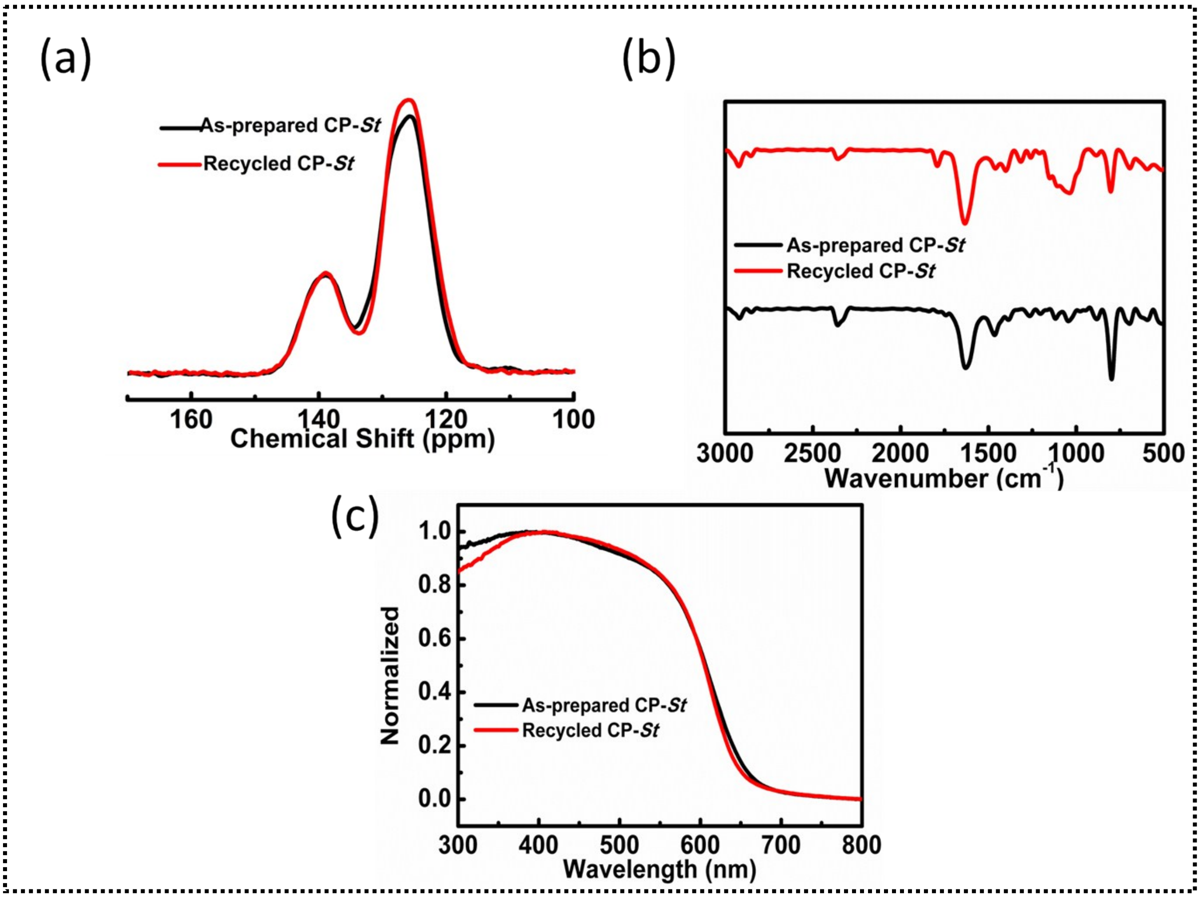

Fig. S24 Solid-state ^{13}C NMR (a) FTIR (b) and Uv-vis (c) spectra of as-prepared and recycled **CP-*St*** from PHP reaction.

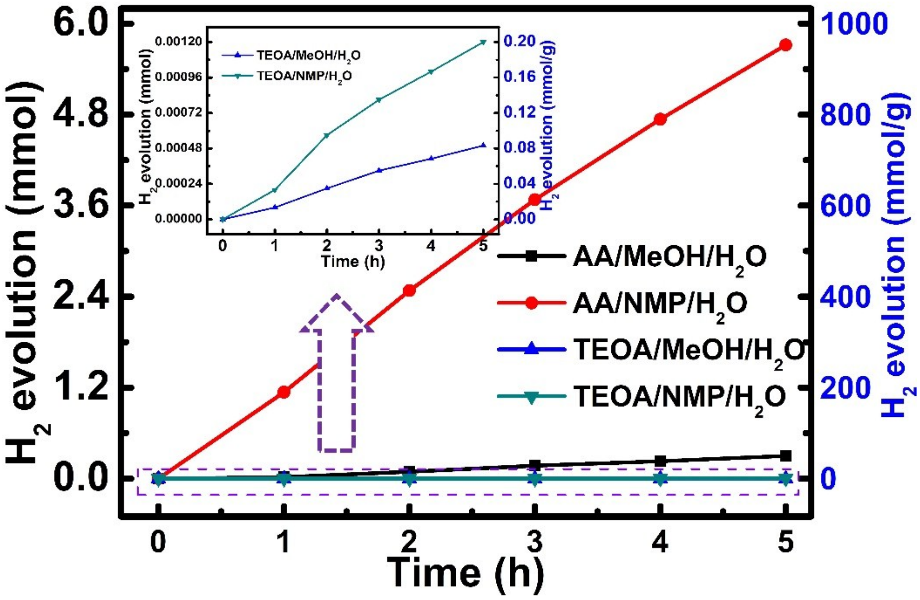

Fig. S25 H_2 evolutions of 6 mg **CP-*St*** dispersed in AA/MeOH/H_2O, AA/NMP/H_2O, TEOA/MeOH/H_2O, and TEOA/NMP/H_2O under visible light irradiation.

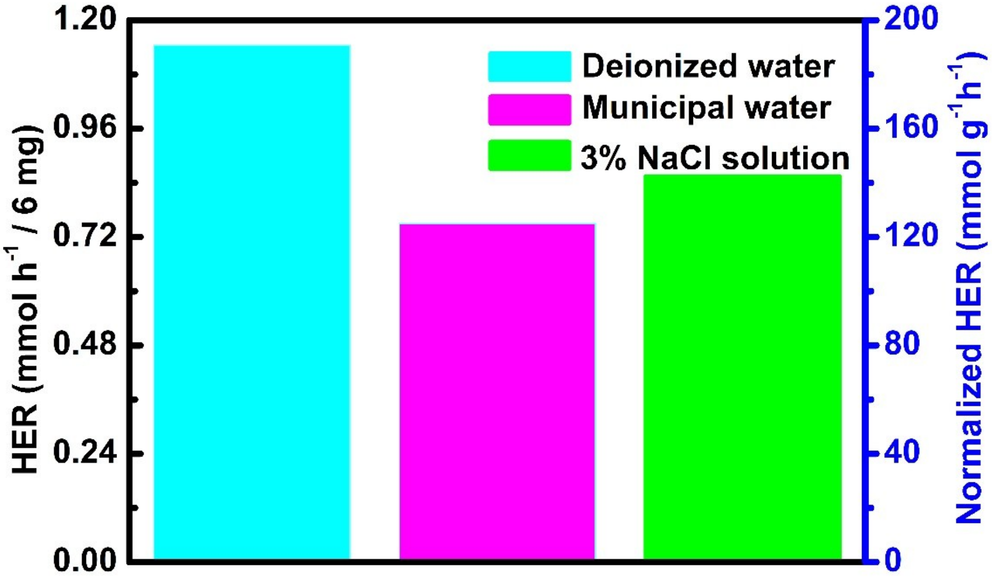

Fig. S26 HERs of **CP-*St***/NMP/AA dispersed in DI water, manicipal water, and simulated seawater.

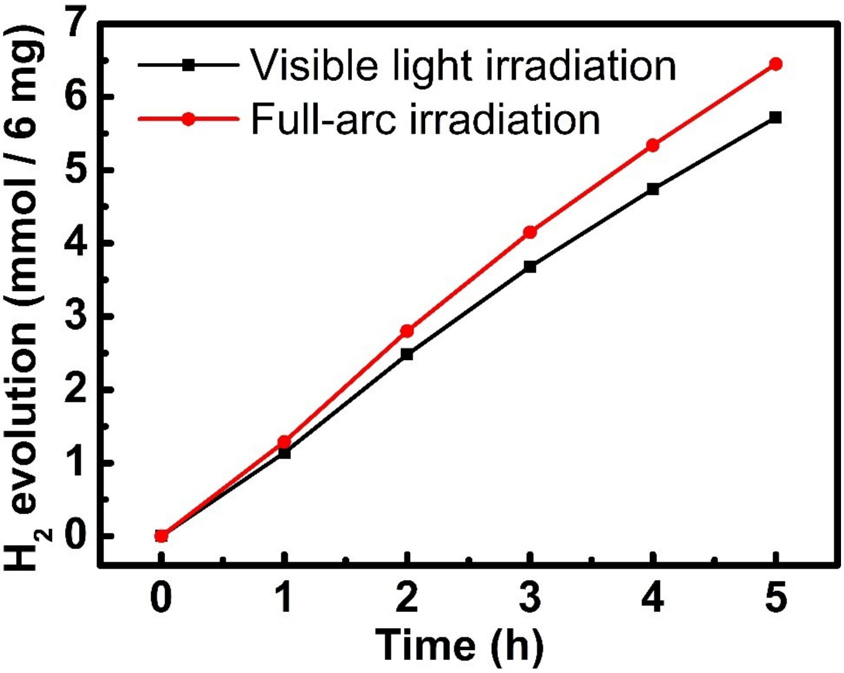

Fig. S27 H_2 evolutions of 6 mg **CP-*St*** dispersed in NMP/H_2O/AA dispersion under visible light irradiation and full-arc irradiation, respectively.

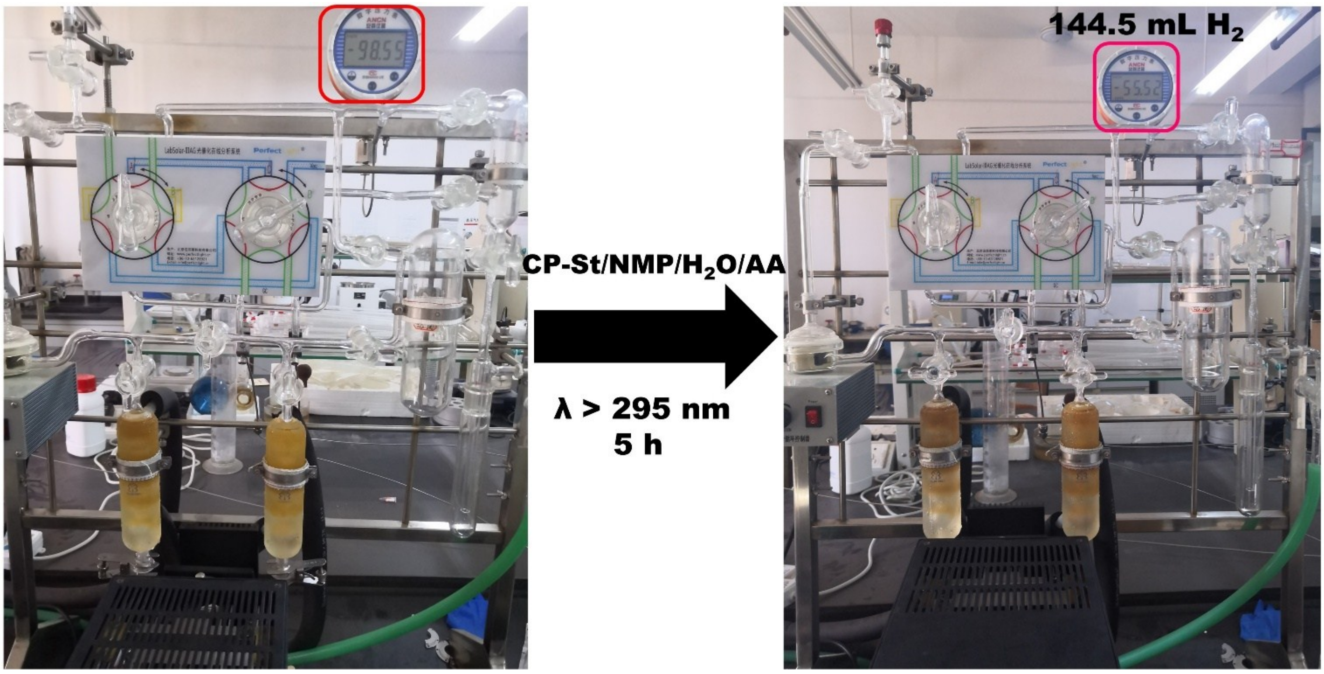

Fig. S28 6.0 mg **CP-*St*** dispersed in NMP/H_2O/AA mixed solution (36 mL, pH =4) under full-arc irradiation for 5 h. [The amount of H_2 were checked by the GC equipped with a TCD detector, and the reading on vacuum gauge before and after irradiation].

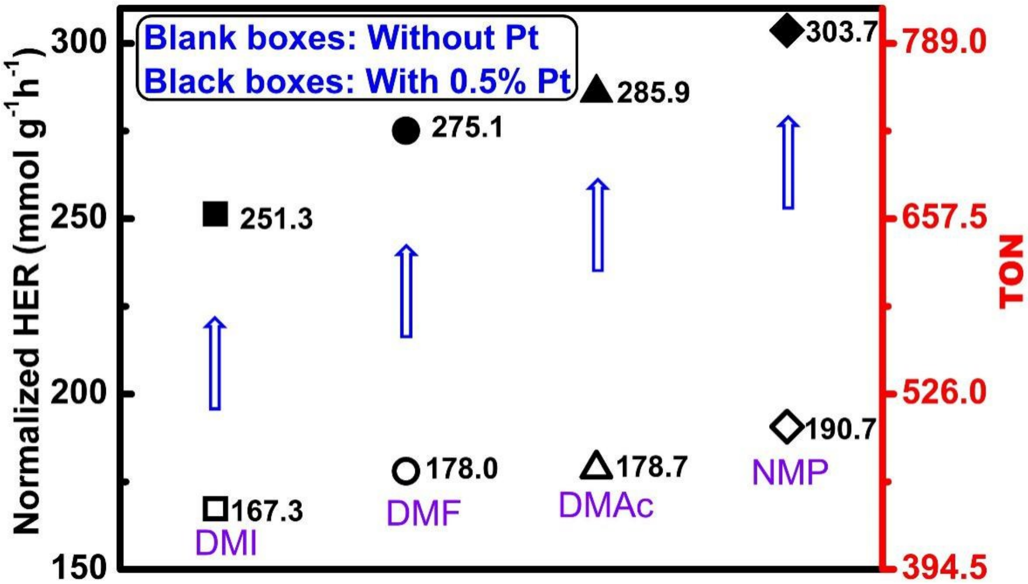

Fig. S29 HERs and TONs of **CP-*St*** dispersed in cosolvents/H_2O/AA, where cosolvents were DMI, NMF, DMAc and NMP respectively, with (■●▲◆) and without (□○△▽) Pt cocatalyst.

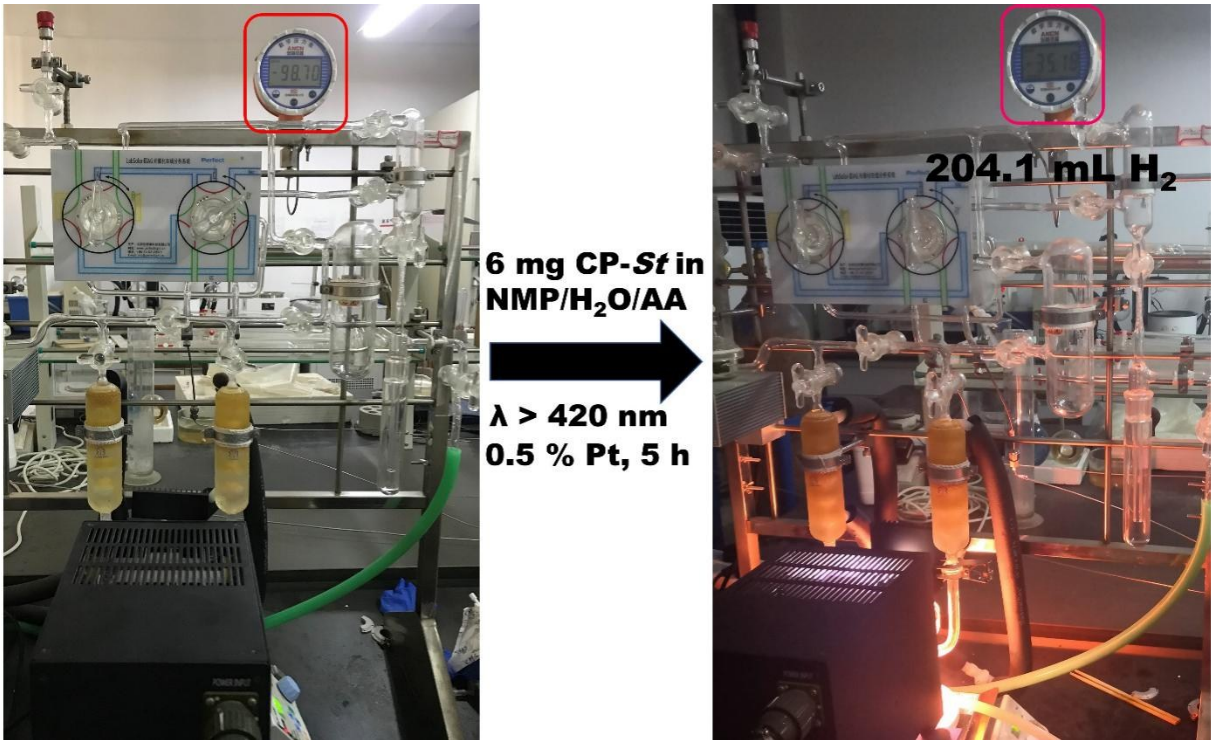

Fig. S30 6.0 mg **CP-*St*** dispersed in NMP/H_2O/AA mixed solution (36 mL, pH =4) and loaded with 0.5% Pt under visible light irradiation for 5 h. [The amount of H_2 were checked by the GC equipped with a TCD detector, and the reading on vacuum gauge before and after irradiation].